Deep-Sea Research I 91 (2014) 72–85

Contents lists available at ScienceDirect

Deep-Sea Research I

journal homepage: www.elsevier.com/locate/dsri

Seasonal dynamics of light absorption by chromophoric dissolved organic matter (CDOM) in the NW Mediterranean Sea (BOUSSOLE site)

Emanuele Organelli [a,b,*], Annick Bricaud [a,b], David Antoine [a,b,c], Atsushi Matsuoka [d]

[a] Sorbonne Universités, UPMC Univ Paris 06, UMR 7093, LOV, Observatoire océanologique, F-06230 Villefranche/mer, France
[b] CNRS, UMR 7093, LOV, Observatoire océanologique, F-06230 Villefranche/mer, France
[c] Curtin University, Department of Imaging and Applied Physics, Remote Sensing and Satellite Research Group, Perth, WA 6845, Australia
[d] Takuvik Joint International Laboratory (CNRS-ULaval), UMI 3376, Département de Biologie and Québec-Océan, Université Laval, Pavillon Alexandre-Vachon, 1045 Avenue de la Médecine, Québec City (Québec), Local 2078, QC, Canada G1V 0A6

ARTICLE INFO

Article history:
Received 20 January 2014
Received in revised form
30 April 2014
Accepted 9 May 2014
Available online 24 May 2014

Keywords:
Chromophoric dissolved organic matter
Light absorption time-series
Photobleaching
Light absorption budget
Mediterranean Sea

ABSTRACT

We analyze a two-year time-series of chromophoric dissolved organic matter (CDOM) light absorption measurements in the upper 400 m of the water column at the BOUSSOLE site in the NW Mediterranean Sea. The seasonal dynamics of the CDOM light absorption coefficients at 440 nm ($a_{cdom}(440)$) is essentially characterized by (i) subsurface maxima forming in spring and progressively reinforcing throughout summer, (ii) impoverishment in the surface layer throughout summer and (iii) vertical homogeneity in winter. Seasonal variations of the spectral dependence of CDOM absorption, as described by the exponential slope value (S_{cdom}), are characterized by highest values in summer and autumn at the surface and low values at the depths of $a_{cdom}(440)$ subsurface maxima or just below them. Variations of $a_{cdom}(440)$ are likely controlled by microbial digestion of phytoplankton cells, which leads to CDOM production, and by photochemical destruction (photobleaching), which leads to CDOM degradation. Photobleaching is also the main driver of S_{cdom} variations. Consistently with previous observations, $a_{cdom}(440)$ for a given chlorophyll *a* concentration is higher than expected from Case I waters bio-optical models. The total non-water light absorption budget shows that surface waters at the BOUSSOLE site are largely dominated by CDOM during all seasons but the algal bloom in March and April. These results improve the knowledge of CDOM absorption dynamics in the Mediterranean Sea, which is scarcely documented. In addition, they open the way to improved algorithms for the retrieval of CDOM absorption from field or satellite radiometric measurements.

1. Introduction

Chromophoric dissolved organic matter (CDOM) is the colored fraction of the organic compounds dissolved in the ocean (DOM). It absorbs solar radiation in the UV and visible ranges of the light spectrum. In contrast to coastal waters where CDOM is mostly delivered by river discharge, CDOM in the open ocean is a mixture of organic substances mainly produced by metabolic activities of autochthonous organisms such as heterotrophic bacteria that recycle phytoplankton cell contents (Coble, 2007). Although CDOM is only a small part of the total DOM in the open sea (Nelson et al., 1998, 2010; Nelson and Siegel, 2002; Siegel et al., 2002), it plays an important role in the carbon cycle (Mopper and Kieber, 2002), and its effect on the bio-optical properties of the water masses is notable. CDOM can contribute more than 50% to the light absorption budget at 440 nm at the surface of the oceans (Bricaud et al., 2002, 2010; Siegel et al., 2002; Babin et al., 2003) and its contribution can increase up to almost 100% below the deep chlorophyll maximum (Bricaud et al., 2010). Because CDOM strongly absorbs in the blue, its varying proportion in the absorption budget confounds classical "blue-to-green" band ratio algorithms for the determination of chlorophyll concentration from remote platforms (Siegel et al., 2005; Morel and Gentili, 2009a). To solve this issue, temporal and spatial dynamics of CDOM optical properties (i.e., light absorption) and their relations with phytoplankton biomass must be investigated.

CDOM light absorption spectra can be expressed as an exponential function as follows (Bricaud et al., 1981):

$$a_{cdom}(\lambda) = a_{cdom}(\lambda_0)\ \exp^{-Scdom(\lambda-\lambda_0)} \quad (1)$$

where $a_{cdom}(\lambda_0)$ (in m^{-1}) is the CDOM absorption coefficient at λ_0, and S_{cdom} (in nm^{-1}) is the exponential slope describing the spectral dependence of absorption. $a_{cdom}(\lambda_0)$ is commonly used

* Corresponding author at: Laboratoire d'Océanographie de Villefranche (LOV), 181 Chemin du Lazaret, 06230 Villefranche sur Mer, France. Tel.: +33 4 93 76 39 11.
E-mail address: emanuele.organelli@obs-vlfr.fr (E. Organelli).

http://dx.doi.org/10.1016/j.dsr.2014.05.003
0967-0637/

as a proxy of CDOM concentration. The S_{cdom} parameter is used as an indicator of CDOM origin (Vodacek et al., 1997) and nature (Carder et al., 1989), or as a tracer of photochemical/microbial degradation processes (Green and Blough, 1994; Moran et al., 2000; Helms et al., 2008). Both $a_{cdom}(\lambda)$ and S_{cdom} are, therefore, the two optical parameters involved in the understanding of CDOM spatial and seasonal dynamics in the world's oceans (Coble, 2007; Nelson and Siegel, 2013).

Several field studies (Babin et al., 2003; Kitidis et al., 2006a; Nelson et al., 2007, 2010; Matsuoka et al., 2007; Bricaud et al., 2010; Swan et al., 2012; Andrew et al., 2013), although analyzing CDOM absorption coefficients at different wavelengths, revealed that $a_{cdom}(\lambda)$ distribution and its relation with chlorophyll *a* concentrations vary temporally and spatially among oceanic basins. This was also confirmed at global scale for the light absorption coefficients of the Colored Detrital Matter (CDM, i.e., CDOM plus Non-Algal Particles) retrieved at 443 nm thanks to satellite-based analyses (Siegel et al., 2002, 2005; Bricaud et al., 2012).

Bricaud et al. (2012) showed that the exponential slope values of CDM also vary among three major oceanic basins and follow specific seasonal dynamics. Regarding the spectral dependence of CDOM absorption, different values were observed between several coastal areas of European seas (Babin et al., 2003) or across the Atlantic (Kitidis et al., 2006a; Andrew et al., 2013) and Southeast Pacific (Bricaud et al., 2010) oceans. Whereas spatial variations in S_{cdom} can reflect variations in chemical composition of the CDOM pool (Carder et al., 1989), temporal modifications are generally driven by biological and chemical processes. Decrease of S_{cdom} values can be observed when CDOM is generated by bacteria (Ortega-Retuerta et al., 2009; Yamashita et al., 2013). Bleaching by solar radiation (i.e., photobleaching) in surface waters degrades CDOM molecules and yields high S_{cdom} and low $a_{cdom}(\lambda)$ values (Vodacek et al., 1997; Nelson et al., 1998; Del Vecchio and Blough, 2002, 2004; Bricaud et al., 2012; Swan et al., 2012).

Based on an analysis using remotely sensed data, Morel and Gentili (2009b) stated that the Mediterranean Sea is characterized by a CDOM content about twice that expected for the same chlorophyll level in other oceanic regions. In addition, they observed a substantial asymmetry of CDOM concentrations between the Western and the Eastern basins that was later confirmed by the investigation of Xing et al. (2012). Despite these findings, the spatial and seasonal dynamics of $a_{cdom}(\lambda)$ and especially of S_{cdom} in the Mediterranean Sea together with their drivers are still poorly understood. This results from the limited number of in situ data both for coastal areas (Seritti et al., 1998; Babin et al., 2003; Vignudelli et al., 2004; Maselli et al., 2009; Para et al., 2010) and for offshore waters (Kitidis et al., 2006b; Bracchini et al., 2010). Only, a recent investigation on light absorption coefficients of CDOM at a single wavelength (412 nm) estimated from fluorometric and radiometric measurements of Bio-Argo floats documented the patterns and drivers of CDOM seasonal dynamics in the open Mediterranean Sea (Xing et al., 2014). The topic is far, however, from being unraveled, and more analyses are needed.

In this study, we present the seasonal dynamics of CDOM at an offshore site in the Mediterranean Sea (BOUSSOLE site; Antoine et al., 2006) as derived from measurements of light absorption coefficients at several wavelengths. The availability of other optical and biological parameters, collected simultaneously with CDOM, represents a unique opportunity to study in depth the drivers of CDOM dynamics for this area. In addition, specific attention is dedicated to the modifications of CDOM spectral characteristics and exponential slope values (S_{cdom}) which are very poorly documented. Considering two years of in situ monthly CDOM measurements, we aim at: (i) investigating seasonal dynamics of CDOM light absorption coefficients at 440 nm and CDOM

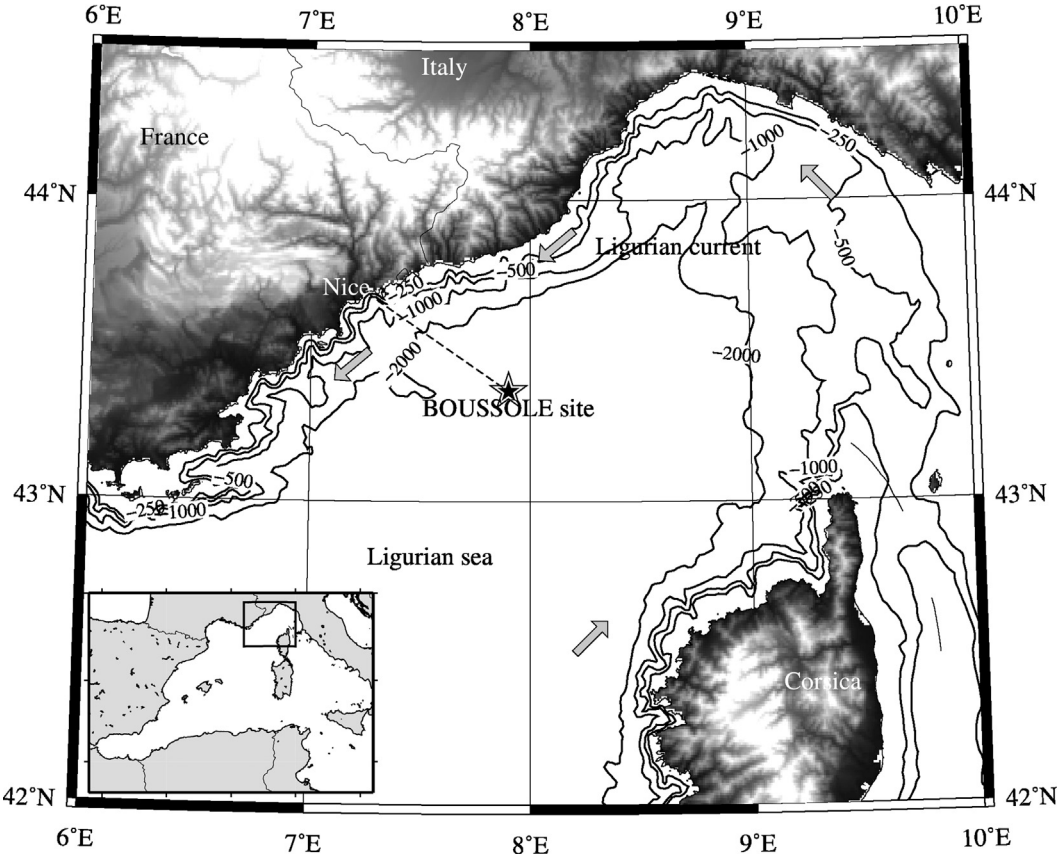

Fig. 1. The NW Mediterranean area where the BOUSSOLE time-series (star) is located.

exponential slope values in the upper 400 m of the water column and analyzing the biological and chemical processes controlling the observed patterns, (ii) assessing relationships between CDOM optical properties and phytoplankton chlorophyll concentrations and finally (iii) evaluating the contribution of CDOM to the total non-water light absorption budget. The data and the analyses here presented contribute to better document the CDOM variability in the Mediterranean Sea. Furthermore, the improved knowledge of CDOM light absorption coefficients and exponential slope values can actually represent useful information for improving inversion algorithms of satellite radiometric measurements in this area.

2. Material and methods

2.1. Study area and sampling

The BOUSSOLE site is located in the Ligurian Sea at approximately 7°54′E, 43°22′N (NW Mediterranean Sea; Fig. 1), about 32 nautical miles off the French Riviera coast (see more details in Antoine et al., 2006) and close to the DYFAMED time-series station (Marty, 2002). Seawater collection was performed monthly in 2011 and 2012 (i.e., Jan. 2011 to Dec. 2012) at generally 12 discrete depths within the 0–400 m water column (5, 10, 20, 30, 40, 50, 60, 70, 80, 150, 200, 400 m). Sampling was carried out by a rosette system equipped with 12-L Niskin bottles. A total of 214 water samples were collected and subsequently used for CDOM light absorption measurements. Water samples were collected also for determining algal pigment and heterotrophic bacteria cells concentrations and for measuring particulate light absorption coefficients. The first optical depth, which defines the thickness of the layer "seen" by an ocean color sensor (Gordon and McCluney, 1975), is a function of the attenuation coefficient of the Photosynthetically Available Radiation (i.e., $1/K_{PAR}$) and was computed for each station as $Z_{eu}/4.6$ (Morel, 1988). The euphotic depth Z_{eu} is the depth at which the PAR is reduced to 1% of its value just below the surface and it was estimated from measured chlorophyll profiles according to Morel and Maritorena (2001). PAR measurements at the surface were also collected every 15 min daily in the 400–700 nm range by a PAR sensor (Satlantic, Inc.) installed on the permanent buoy located at the BOUSSOLE site (Antoine et al., 2006). Vertical temperature and salinity profiles were recorded monthly using a SeaBird SBE 911-plus CTD equipped with sensors for pressure (Digiquartz Paroscientific), temperature (SBE3+) and conductivity (SBE4). After determination of density, the Mixed Layer Depth (MLD) was computed as the depth where the difference from density at 10 m was 0.125 kg m^{-3}.

2.2. CDOM absorption measurements

Water samples were filtered immediately after sampling into glass bottles, in dim light, using pre-rinsed 0.2 µm GHP filters (Acrodisc Inc.). Filtered samples were kept refrigerated and warmed at room temperature at the time of the analysis. All measurements were performed within 24 h after sampling, following the Ocean Optics Protocols (Mitchell et al., 2002).

CDOM absorption measurements were performed using a multiple path length, liquid core waveguide, UltraPath (World Precision Instruments, Inc.). The detailed methodology for absorption measurements is described in Bricaud et al. (2010) and Matsuoka et al. (2012). Briefly, filtered samples were pumped into the capillary tube of the Ultrapath instrument using a peristaltic pump, and absorbance spectra were measured between 250 and 735 nm with 1 nm increments, with reference to a salt solution (38 g L^{-1}) prepared with Milli-Q water and granular NaCl precombusted in an oven (at 450 °C for 4 h). The maximum path length (200 cm) was used for all samples. Between each sample, the capillary tube was flushed successively with diluted solutions of detergent (5%), high reagent grade MeOH (50%), 2 M HCl, and Milli-Q water, and the cleanliness of the tube was checked by recording the absorption spectrum of reference water.

Care was taken to avoid the presence of bubbles during measurement, so that absorbance values in the red part of the spectrum were always 0 or very close to 0. All measured spectra were corrected for residual absorbance, if any, by assuming that the average of measured values over a 5 nm interval around 685 nm must be 0, and shifting the spectra accordingly (samples were disregarded if this value was > 0.02 AU; for 67% of samples it was < 0.005 AU). Finally, the corrected absorbance spectra (n=210; 34 within the first optical depth) were converted into absorption coefficients, $a_{cdom}(\lambda)$ (in m^{-1}). For each spectrum, the spectral slope, S_{cdom} (in nm^{-1}), was computed by applying a non-linear least-square fit to the $a_{cdom}(\lambda)$ values between 350 and 500 nm (Babin et al., 2003).

2.3. Pigment measurements

Chlorophyll *a* concentrations were measured together with other algal pigments by high performance liquid chromatography (HPLC). Seawater samples (2.8 L) were filtered through 25 mm GF/F Whatman filters and immediately stored in liquid nitrogen and then in a −80 °C freezer in the laboratory until analysis. The HPLC procedure applied here is fully described in Ras et al. (2008). This method showed a lowest detection limit of 0.0001 mg m^{-3} for chlorophyll *a* which corresponds to a *S*/*N* ratio equal to 3. The sum of concentrations of chlorophyll *a*, divinyl chlorophyll *a*, chlorophyllide *a*, pheophorbide *a*

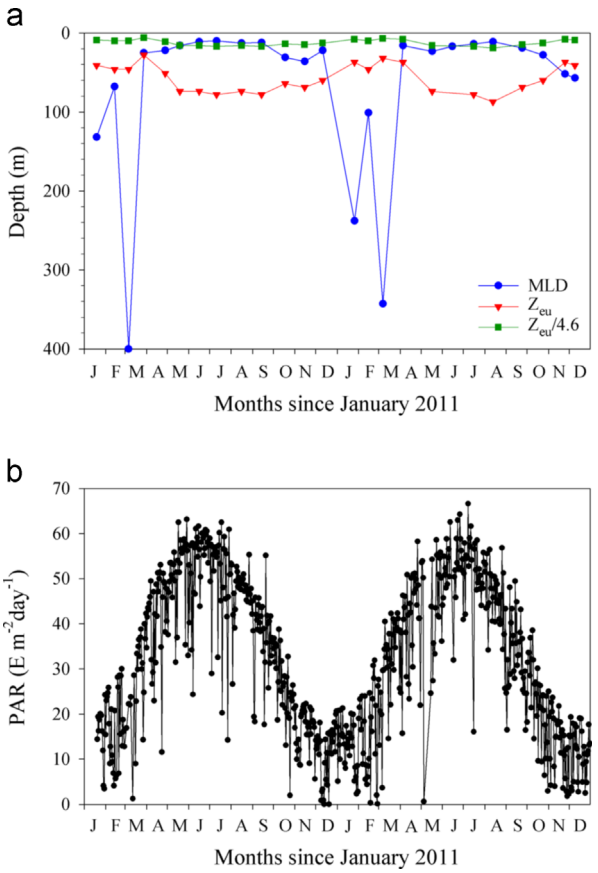

Fig. 2. Time-series of hydrological and optical parameters measured at the BOUSSOLE site from January 2011 to December 2012: (a) Mixed Layer Depth (MLD), euphotic depth (Z_{eu}) and first optical depth (Z_{eu}/4.6); (b) daily PAR values.

and pheophytin *a* is used here as index of phytoplankton biomass and noted [Tchl *a*+pheo *a*].

2.4. Flow cytometry analyses

Seawater samples (2 mL) were immediately fixed after sampling with a solution of glutaraldehyde (1%). Samples were stored in the dark at 4 °C for 15 min and then frozen in liquid nitrogen on board and in a −80 °C freezer in the laboratory until analysis. Measurements of heterotrophic bacteria cell concentrations were performed by a flow cytometer FACSCANTO II (BD Biosciences) at the Observatoire Océanologique de Banyuls sur Mer (France). Before counting, cells were marked by a fluorochrome (SyberGreenI) specific for nucleic acids. Flow cytometry measurements were available only during 1 year of the time-series (i.e., Dec. 2011 to Dec. 2012).

2.5. Particulate absorption measurements

Particulate light absorption spectra, $a_p(\lambda)$, were measured by the "quantitative filter pad technique (QFT)" (Mitchell, 1990; Mitchell et al., 2000). Seawater for each sample (2.8 L) was filtered through a 25 mm Whatman GF/F filter, immediately frozen in liquid nitrogen and subsequently stored in laboratory at −80 °C until analysis. Spectra were measured from 300 to 800 nm with 1 nm increments using a spectrophotometer Lambda 850 (Perkin–Elmer) equipped with an integrating sphere. A blank wet filter was used as a reference. Measured optical densities were shifted to 0 in the near infrared before being transformed into absorption coefficients (in m^{-1}). All spectra ($n=186$) were corrected for the path length amplification factor (β) according to Bricaud and Stramski (1990). Finally, the particulate absorption spectra were decomposed into phytoplankton, $a_{phy}(\lambda)$, and non-algal particles, $a_{NAP}(\lambda)$, absorption coefficients using the numerical decomposition technique of Bricaud and Stramski (1990).

3. Results and discussion

3.1. Physical environment

Hydrological and optical conditions of the water column at the BOUSSOLE site over the period 2011–2012 are shown in Fig. 2. As already observed for the Western basin of the Mediterranean Sea

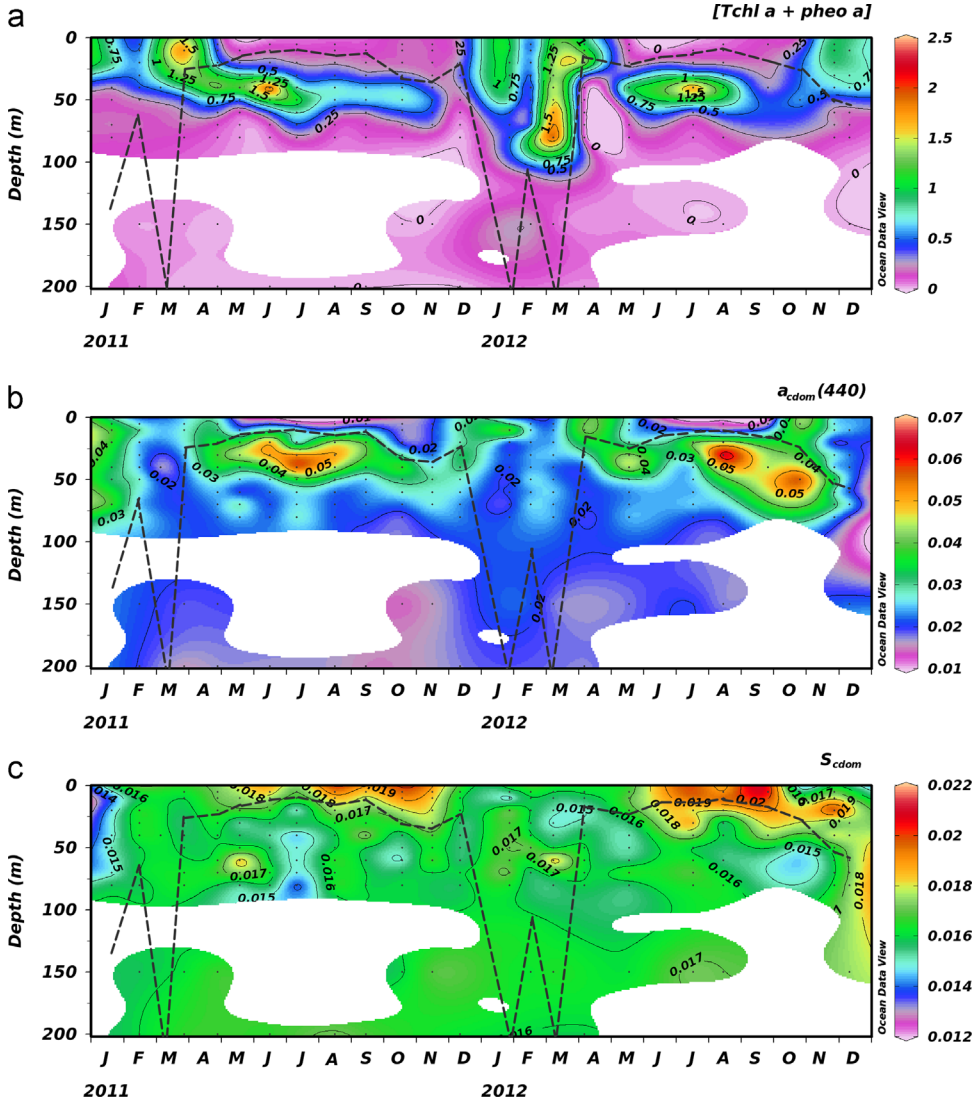

Fig. 3. Contour plots of (a) total chlorophyll *a* plus pheopigment *a* concentrations ([Tchl *a*+pheo *a*], mg m^{-3}); (b) CDOM absorption coefficients at 440 nm ($a_{cdom}(440)$, m^{-1}); (c) CDOM exponential slope values (S_{cdom}, nm^{-1}). Data are displayed within 0–200 m ($n=199$) for the period from January 2011 to December 2012. Small dots represent samples collected during each cruise and the dashed line indicates the Mixed Layer Depth (MLD). Note that stratification of [Tchl *a*+pheo *a*] in March 2011, when MLD is > 200 m, is likely an artefact induced by the lack of samples in the layer below 50 m. The map is drawn by the Ocean Data View software (Schlitzer, R., Ocean Data View, http://odv.awi.de, 2012).

(Marty et al., 2002; D'Ortenzio et al., 2005), strong seasonality exists in the mixed layer depth variations (Fig. 2a). Deep mixed layers (from 70 up to 400 m) characterized wintertime. Stratification of the water column began in spring and shallowest MLD values (around 11–12 m) were reached in summer. Here and throughout the paper, seasons are defined as winter (21/12–20/3), spring (21/3–20/6), summer (21/6–21/9) and autumn (22/9–20/12). Daily PAR values at the surface were generally around 10–30 E m^{-2} day^{-1} during winter. They increased up to 67 E m^{-2} day^{-1} in summer (Fig. 2b). Shallow euphotic layers were observed in winter (32 m $< Z_{eu} <$ 46 m) while the deepest ones characterized the water column at the end of the spring and in summertime (74 m $< Z_{eu} <$ 87 m; Fig. 2a). The surface layer, limited at the first optical depth (Z_{eu}/4.6), obviously followed a similar dynamics with minimal values of Z_{eu}/4.6 (around 7–10 m) in winter and maximal values (16 m $< Z_{eu}$/4.6 $<$ 19 m) during spring and summer (Fig. 2a).

3.2. Seasonal variations of total chlorophyll a

Two-year time-series of total chlorophyll *a* concentration ([Tchl *a*+pheo *a*]) at the BOUSSOLE site and its seasonal patterns are shown in Fig. 3a and Fig. 4a–d, respectively. During winter, when deep convective water mixing occurred, [Tchl *a*+pheo *a*] was high and homogeneously distributed within the 0–80 m layer (0.75 ± 0.53 mg m^{-3}) while it rapidly decreased to a value close to 0 below 80 m (Fig. 4a). The spring bloom (0.99–1.84 mg m^{-3}) formed at 5–10 m between March and April (Fig. 3a), as already observed (Marty et al., 2002; Organelli et al., 2013). From the middle of spring (May), [Tchl *a*+pheo *a*] concentrations at 5–10 m gradually

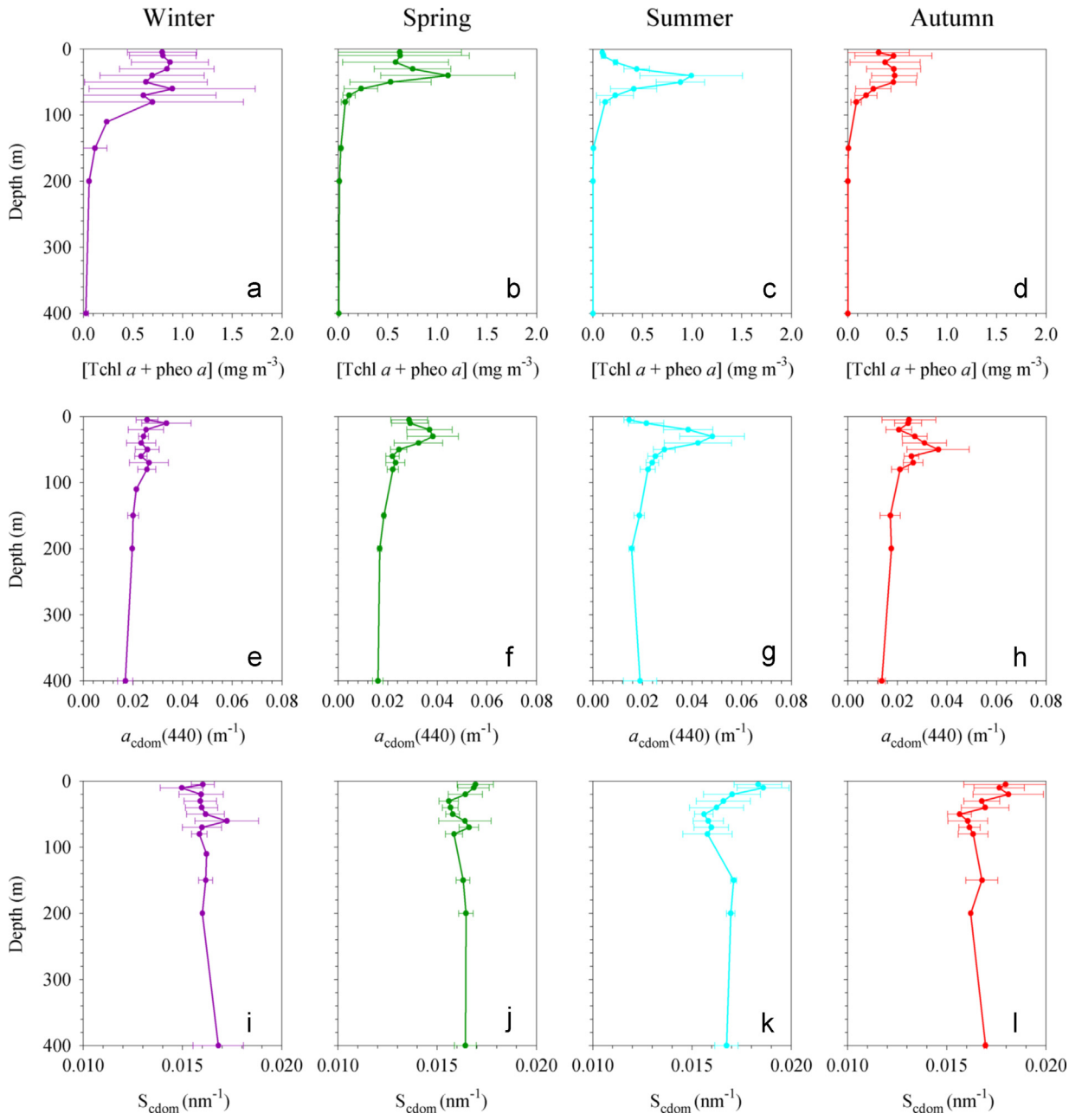

Fig. 4. Seasonal mean profiles (plus standard deviations) of (a)–(d) total chlorophyll *a* plus pheopigment *a* concentrations ([Tchl *a*+pheo *a*]); (e)–(h) CDOM absorption coefficients at 440 nm ($a_{cdom}(440)$); (i)–(l) CDOM exponential slope values (S_{cdom}). Each profile includes 2–3 months of measurements.

decreased to values of 0.10 ± 0.02 mg m^{-3} in summertime (Figs. 3a and 4c), as a result of depletion of nutrients due to the strong stratification of the water column (Marty et al., 2002). At the same time, a deep chlorophyll maximum (DCM) formed at approximately 40 m depth and reinforced throughout summer (Fig. 4b and c). Highest DCM values were observed in June 2011 (2.11 mg m^{-3}) and July 2012 (1.84 mg m^{-3}) (see Fig. 3a). Chlorophyll-depleted surface waters and a weak DCM (0.47 ± 0.23 mg m^{-3}) persisted in autumn (Fig. 4d) until vertical mixing homogenized chlorophyll concentration along the water column.

3.3. Seasonal variations of CDOM light absorption at 440 nm

CDOM absorption coefficients at 440 nm ($a_{cdom}(440)$) showed a clear seasonal dynamics within the 0–200 m layer at the BOUSSOLE site in 2011 and 2012 (Fig. 3b). In this layer, $a_{cdom}(440)$ was homogeneously distributed during winter (0.025 ± 0.006 m^{-1}; Fig. 4e). Then, $a_{cdom}(440)$ values up to 0.04 m^{-1} were observed at 5 and 10 m in March and April and again in October and November (Fig. 3b). A strong reduction of surface $a_{cdom}(440)$ values was observed from spring to summer, as vertical stratification and daily surface PAR increased (Fig. 2): at 5 m, $a_{cdom}(440)$ values decreased from 0.029 ± 0.007 m^{-1} in spring to 0.015 ± 0.002 m^{-1} in summer (Fig. 4f and g). $a_{cdom}(440)$ maxima formed at 30 m depth in spring (0.038 ± 0.010 m^{-1}; Fig. 4f) and reinforced throughout summer (0.048 ± 0.013 m^{-1}; Fig. 4g). A maximum of CDOM absorption (0.036 ± 0.012 m^{-1}) was also found in autumn but in deeper waters (50 m; Fig. 4h).

The seasonal cycle of CDOM absorption at BOUSSOLE is similar to that described at the Bermuda Atlantic Time-Series study (BATS) site in the Sargasso Sea for CDOM absorption coefficients at 300 nm (Nelson et al., 1998) and 325 nm (Nelson and Siegel, 2013), with three main features: (i) subsurface maxima forming in spring and progressively reinforcing throughout summer, (ii) impoverishment in the surface layer throughout summer and (iii) vertical homogeneity in winter. In addition, CDOM seasonal patterns at the surface were consistent also with the observations in the Mediterranean Sea of the light absorption coefficients derived from measurements by Bio-Argo floats at 412 nm (Xing et al., 2014) and SeaWiFS imagery at 443 nm (Bricaud et al., 2012).

Considering the $a_{cdom}(440)$ values observed within the first optical depth (0.012–0.044 m^{-1}), good agreement with the estimates of CDM absorption at 443 nm derived from SeaWiFS data over the entire Mediterranean Sea (0.006–0.043 m^{-1}; Bricaud et al., 2012) was found. Also, CDOM absorption coefficients at 412 nm measured in May at 5–10 m (0.039 ± 0.006 m^{-1}, $n=3$) were similar to those retrieved from fluorometric and radiometric measurements recorded by the Bio-argo float "MED_NW_B02" (see for details Xing et al., 2012, 2014) within 3 km from the BOUSSOLE site in May 2008 (0.042 ± 0.002 m^{-1}, $n=8$; X. Xing, personal communication). Besides this study, very few CDOM absorption measurements in the Mediterranean Basin are available for comparison. CDOM absorption coefficients at 300 nm at the BOUSSOLE site in May (0.41 ± 0.07 m^{-1}, 0–30 m, $n=7$) were significantly higher ($p < 0.001$) than values reported by Kitidis et al. (2006b) for the Cyprus gyre in the Eastern Mediterranean

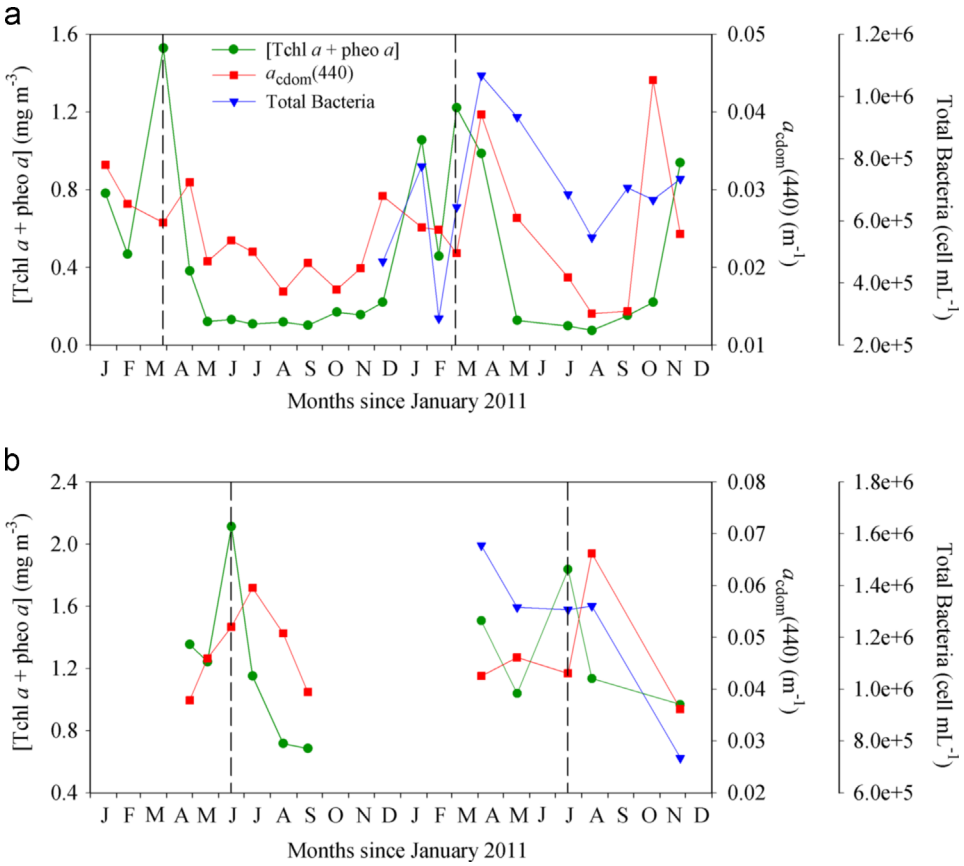

Fig. 5. (a) Time-series of total chlorophyll *a* plus pheopigment *a* concentrations ([Tchl *a*+pheo *a*]), CDOM absorption coefficients at 440 nm ($a_{cdom}(440)$) and total heterotrophic bacteria concentrations in the first optical depth at the BOUSSOLE site. Values displayed are the average of concentrations measured at 5 and 10 m. (b) as in (a) but for the maximal values of the three parameters as found below the first optical depth. Dashed line indicates the time of maximal total chlorophyll *a* plus pheopigment *a* concentration.

($0.25 \pm 0.04\ m^{-1}$, 0–30 m, $n=46$). The CDOM absorption coefficients at 300 nm in November at the BOUSSOLE site ($0.35 \pm 0.04\ m^{-1}$, 0–40 m, $n=10$) were, instead, lower than values reported by Bracchini et al. (2010) for the central eastern Mediterranean Sea ($0.39 \pm 0.05\ m^{-1}$, 0–40 m, $n=14$). Although CDOM content is expected to be asymmetric between the sub-basins of the Mediterranean (Morel and Gentili, 2009b; Xing et al., 2012), these divergences may also be due to methodological differences. Indeed, Kitidis et al. (2006b) and Bracchini et al. (2010) used a 10-cm path length and pure water as a reference.

3.4. Seasonal variations of CDOM exponential slope

Figs. 3c and 4i–l display the 0–200 m distribution of S_{cdom} and its seasonal patterns at the BOUSSOLE site in 2011 and 2012. Analogously to $a_{cdom}(440)$, S_{cdom} values were rather constant along the water column during winter ($0.016 \pm 0.0009\ nm^{-1}$, Fig. 4i). An increase of S_{cdom} values was observed at 5–10 m depth from spring ($0.017 \pm 0.0007\ nm^{-1}$) to summer ($0.0185 \pm 0.001\ nm^{-1}$) and autumn ($0.018 \pm 0.002\ nm^{-1}$). During summer and autumn, S_{cdom} in subsurface waters (below 20 m depth) decreased to values lower than $0.015\ nm^{-1}$ at the depths of $a_{cdom}(440)$ subsurface maxima or just below them (Fig. 3c).

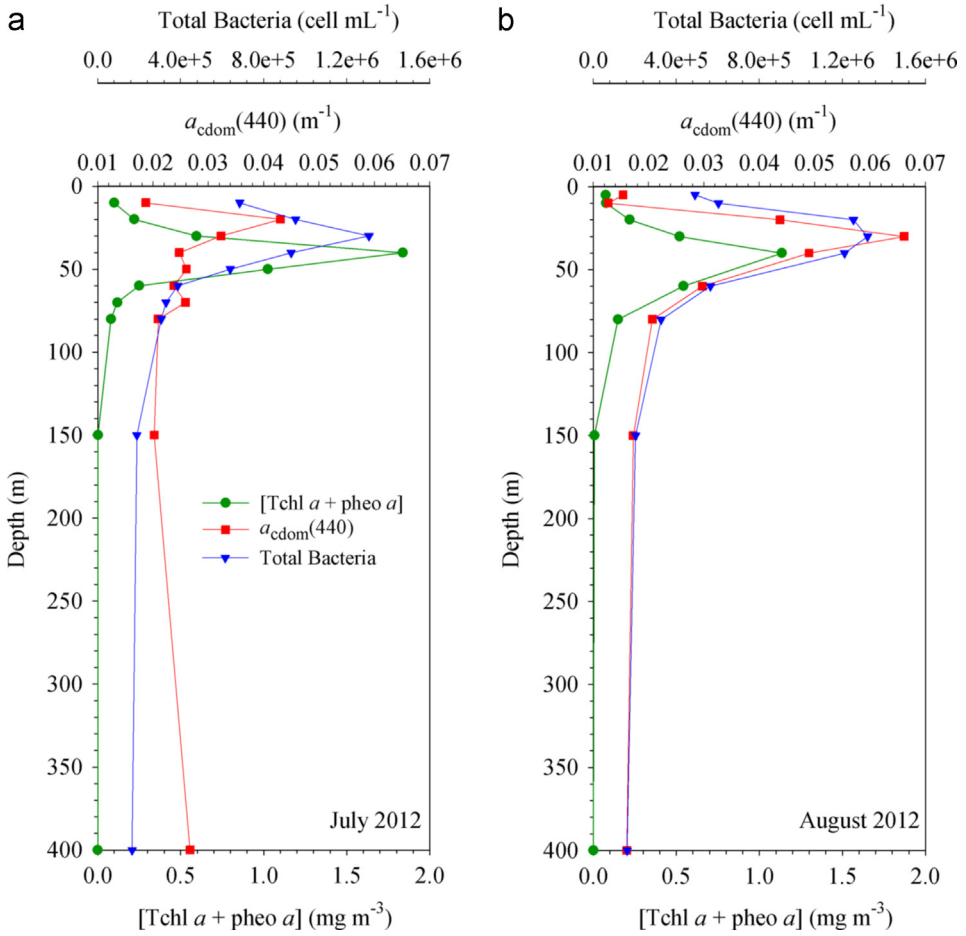

Fig. 6. Vertical profiles of total chlorophyll *a* plus pheopigment *a* concentrations ([Tchl *a*+pheo *a*]), CDOM absorption coefficients at 440 nm ($a_{cdom}(440)$) and total heterotrophic bacteria concentrations in (a) July 2012 and (b) August 2012.

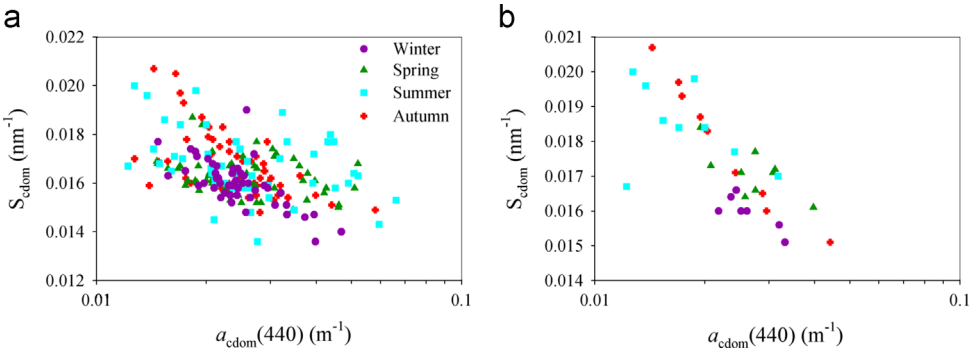

Fig. 7. Variations of CDOM exponential slope values (S_{cdom}) as a function of CDOM absorption coefficients at 440 nm ($a_{cdom}(440)$): (a) for all depths ($n=210$) and (b) within the first optical depth ($n=34$).

S_{cdom} values in the surface layer were consistent with previous estimations from in situ and satellite remote sensing measurements in the Mediterranean Sea. S_{cdom} values at BOUSSOLE varied from 0.015 to 0.021 nm^{-1} and fell within the range of values observed for CDM by Bricaud et al. (2012) in the Mediterranean Sea (0.015–0.03 nm^{-1}). In addition, the average value computed for the surface layer regardless of the season (0.0175 ± 0.0015 nm^{-1}) was close to that found by Babin et al. (2003) in Mediterranean waters (0.017 ± 0.0028 nm^{-1}). S_{cdom} values calculated over the 270–400 nm range at the BOUSSOLE site in November (0.025 ± 0.004 nm^{-1}, 0–40 m, $n=10$) were, instead, significantly lower ($p<0.001$) than values reported by Bracchini et al. (2010) for the central eastern Mediterranean Sea (0.038 ± 0.002 nm^{-1}, 0–40 m, $n=14$). Whereas such discrepancy could be also related to the chemical composition of CDOM (Carder et al., 1989), it is more likely due to the methodological differences in CDOM measurements (see Section 3.3).

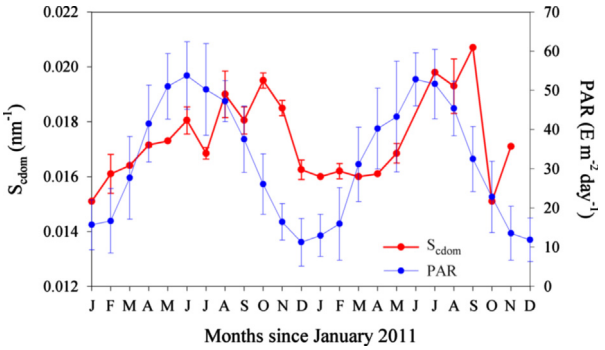

Fig. 8. Monthly means (plus standard deviations) of CDOM exponential slope values (S_{cdom}; bold line) within the first optical depth and surface daily PAR (thin line) measured at the BOUSSOLE site in 2011 and 2012.

3.5. Control of CDOM seasonal patterns

CDOM seasonal patterns are essentially controlled by modifications of the water column physical structure and by the balance between production and degradation processes (Coble, 2007). Previous field studies suggested that CDOM is essentially a by-product of heterotrophic microbial degradation of phytoplankton cells rather than a direct product of algal metabolism (Nelson et al., 1998, 2004; Rochelle-Newall and Fisher, 2002). The contribution of phytoplankton to the production of CDOM through cellular exudation has been, however, recently observed in laboratory experiments (Romera-Castillo et al., 2010). The importance of microbial activity in this process was shown by a simple model of CDOM production as a function of heterotrophic bacterial production and photochemical destruction at the BATS site (Nelson et al., 1998). At the BOUSSOLE site, a multiple regression analysis showed that microbes were primarily responsible for CDOM production ($p<0.05$). The involvement of bacteria in this process was also suggested by the temporal and spatial relationships (Figs. 5 and 6, respectively) between CDOM absorption coefficients, total chlorophyll *a* and total heterotrophic bacteria concentrations. Annual maxima of CDOM absorption coefficients occurred generally 1 month (approximately 25–31 days) later than the spring bloom at the surface (Fig. 5a) and the DCM in summer (Fig. 5b) but simultaneously with high bacterial abundance. Cross-correlation analysis confirmed the occurrence of 1-month lag between CDOM and chlorophyll with correlation coefficients of 0.46 ($p<0.05$) for the time-series at the surface and 0.74 ($p<0.05$) at the DCM. Because the BOUSSOLE site is sampled monthly, the lag between CDOM and chlorophyll in spring and summer cannot be studied over shorter time windows. This outcome, however, is in agreement with a previous study based on remote sensing observations (Hu et al., 2006). These authors observed that CDOM lagged chlorophyll by 2 to 5 weeks in the southern Sargasso Sea as a consequence of phytoplankton degradation. Analysis of the vertical profiles of total chlorophyll *a*, CDOM absorption coefficients and total bacteria concentrations (Fig. 6) also highlighted the involvement of bacteria in CDOM production. Vertical distributions of the three parameters during two summer months, July 2012 (DCM maximum) and August 2012 (CDOM maximum), are shown as examples in Fig. 6. CDOM and bacteria subsurface maxima were generally at the same depth (e.g., August 2012) and always above the DCM by at least 10 m (Fig. 6). It is important, however, to keep in mind that the post-bloom production of CDOM cannot be ascribed only to heterotrophic bacteria. Recent investigations in the Atlantic Ocean (Kitidis et al., 2006a) and in the Mediterranean Sea (Xing et al., 2014) suggested the presence of bacterial activities coupled to planktonic food web interactions (sloppy feeding) as CDOM end-members. This latter viewpoint was essentially demonstrated by incubation experiments on several zooplankton species collected in the North Atlantic Ocean (Steinberg et al., 2004) that proved excretion processes by zooplanktonic grazers to be one source of CDOM in open ocean.

Photobleaching was likely the main cause of CDOM destruction in the surface layer from spring to summer at the BOUSSOLE site, as generally observed for other oceanic waters (Nelson et al., 1998, 2010; Coble, 2007; Bracchini et al., 2010; Swan et al., 2012). Photobleaching transforms compounds with high molecular weight into low-weight molecules that absorb light in the shorter spectral domain, resulting in an increase of S_{cdom} (Twardowski et al., 2004; Helms et al., 2008). The inverse relationship between S_{cdom} and $a_{cdom}(440)$ was evident ($r^2=0.60$; $p<0.0001$; $n=34$) within the first optical depth at the BOUSSOLE site (Fig. 7b) while a high scatter was observed in the relation between S_{cdom} and $a_{cdom}(440)$ all along the water column ($r^2=0.14$; $p<0.0001$; $n=210$; Fig. 7a). As expected, photobleaching was strongest in the surface layer. The sun-induced CDOM degradation occurred especially during summer and autumn, when very low CDOM absorption coefficients and high S_{cdom} values were observed (Fig. 7b). The S_{cdom} highest values occurred in October 2011 and September 2012, i.e., near the end of the thermal stratification period and more than 3 months after the maximal PAR values in June (Fig. 8). This time lag between PAR and S_{cdom} values may suggest that CDOM photoreactivity is not necessarily related to highest solar radiation rates, but it is more likely dependent on the time of exposure to light. The photochemical lability of CDOM was found to depend on the accumulated exposure to light (Yamashita et al., 2013) and on the light history of the water column (Swan et al., 2012). Swan et al. (2012) observed that CDOM susceptibility to solar-induced destruction can also vary according to the photo-oxidative and biogeochemical conditions of the water column (i.e., nitrate concentrations).

3.6. Variations of CDOM spectral features

CDOM spectra found in oceanic waters are usually featureless (Nelson et al., 1998, 2007; Swan et al., 2009; Yamashita and Tanoue, 2009). Many CDOM spectra at the BOUSSOLE site showed, however, bumps of absorption around 410–420 nm and 310–320 nm (Fig. 9). The absorption bump at 410–420 nm was previously found in the Pacific and Atlantic Oceans (e.g., Bricaud et al., 2010; Röttgers and Koch, 2012) while that at 310–320 nm was observed in Antarctic waters (Norman et al., 2011). The absorption bump around 410–420 nm was frequently observed in samples collected below the first optical depth regardless of the season (Fig. 9b, d, f, h), and in spectra from surface waters in winter (Fig. 9a). At the surface, this absorption bump was also occasionally observed in spring and autumn but never in summer (Fig. 9e).

The bump around 310–320 nm was observed at several depths in the 0–400 m layer but only in autumn (Fig. 9g and h).

Two different hypotheses from previous studies (Bricaud et al., 2010; Röttgers and Koch, 2012) can be taken into consideration to explain the origin of the absorption bump at 410–420 nm. Bricaud et al. (2010), for instance, speculated that the occurrence of this feature in waters of the Southeast Pacific ocean could be due to the presence of pheopigments released by the cells. In effect, an increasing trend of the bump height with pheopigment concentrations was observed when analyzing the BOUSSOLE dataset, but with very high scatter ($r^2=0.07$, $p<0.001$, $n=210$). This suggested the contribution of other absorbing pigments to this bump. Indeed, Röttgers and Koch (2012) ascribed the occurrence of this feature to a non-chlorin metal-free porphyrin derived from degradation of complex molecules such as hemes, cytochromes and chlorophyll *c*. However, Röttgers and Koch (2012) observed these compounds at the DCM and below 100 m, while at the BOUSSOLE site the bump of absorption was found at every depth below 20 m.

The bump of CDOM absorption around 310–320 nm could be due to the presence of mycosporine-like amino acids (MAAs), in agreement

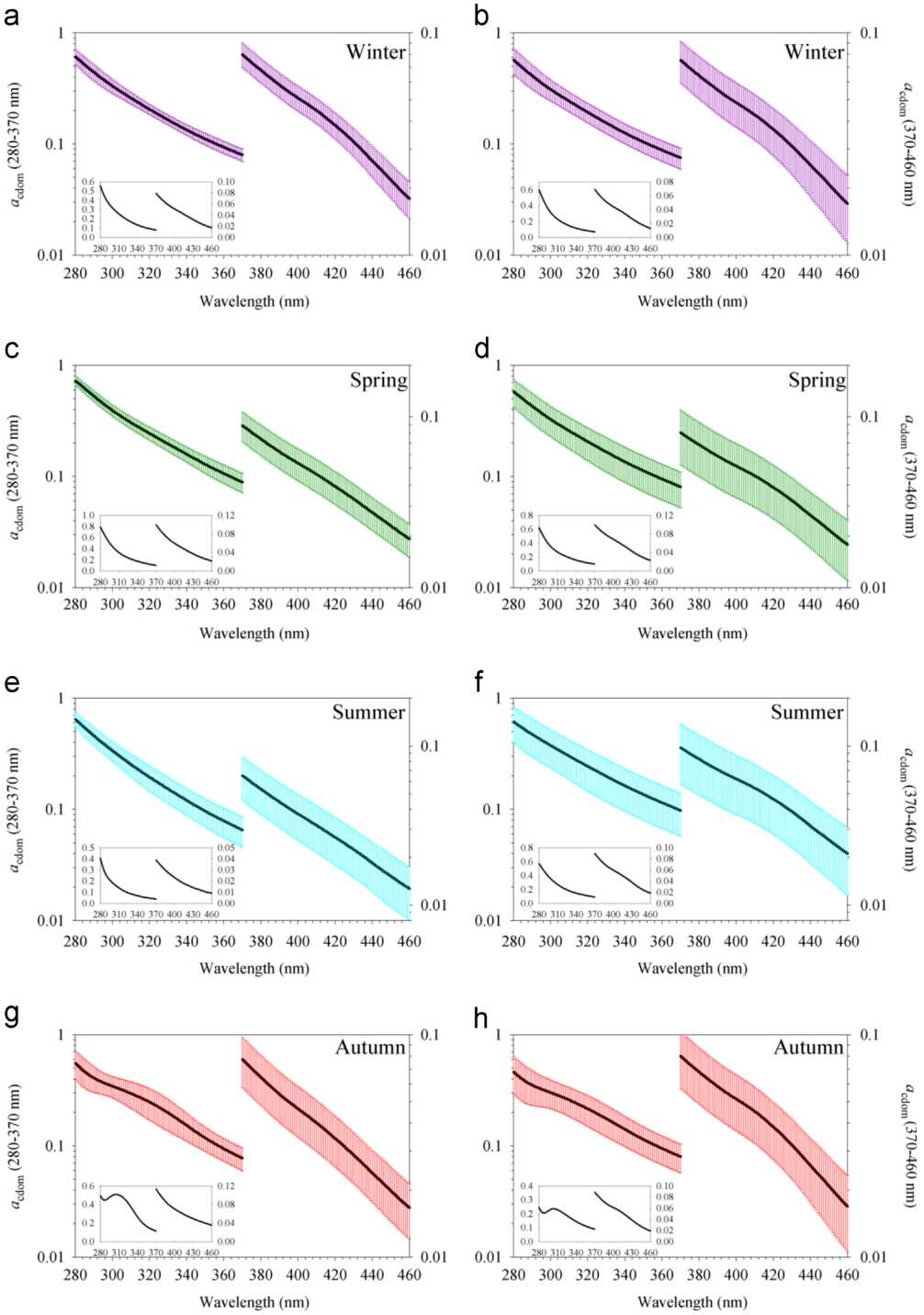

Fig. 9. Seasonal averages (plus standard deviations) of CDOM absorption spectra (m^{-1}; lin-log scale): (a), (c), (e), (g) within the first optical depth; (b), (d), (f), (h) below the first optical depth. In each inset, a measured CDOM absorption spectrum is displayed (linear scale) as an example. Spectra are displayed for the ranges 280–370 nm and 370–460 nm.

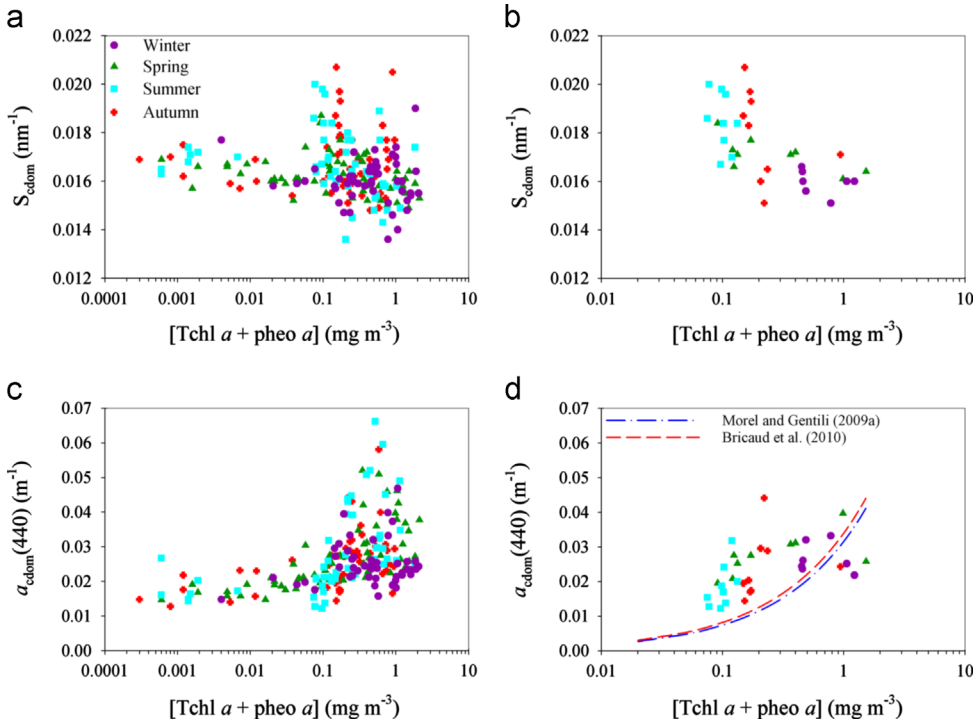

Fig. 10. (a) Variations of the CDOM exponential slope (S_{cdom}) as a function of [Tchl a+pheo a] at the BOUSSOLE site for the 0–400 m water column (n=210); (b) as in (a) but for the first optical depth only (n=34). (c) Variations of the CDOM absorption coefficients at 440 nm (a_{cdom}(440)) as a function of [Tchl a+pheo a] at the BOUSSOLE site for the 0–400 m water column (n=210); (d) as in (c) but for the first optical depth only (n=34). In panel (d) regression lines from Morel and Gentili (2009a) and Bricaud et al. (2010) are displayed.

with previous findings (Whitehead and Vernet, 2000; Steinberg et al., 2004; Tilstone et al., 2010; Norman et al., 2011). This large group of compounds is characterized by a light absorption maximum between 310 and 360 nm depending on their chemical nature (Carreto and Carignan, 2011). They are produced to protect photosynthetic systems from high irradiance exposure, and were found within several algal classes and particularly in cyanobacteria (Carreto and Carignan, 2011). Previous studies in the Ligurian Sea observed maximal abundance of picophytoplankton and mostly cyanobacteria during summer and at the end of the period of stratification (Marty et al., 2002; Organelli et al., 2013), which suggests intra-cellular MAAs production by these organisms during this period. Maxima around 320 nm were actually observed on the phytoplankton light absorption spectra, in particular for surface samples. However, at the BOUSSOLE site, summer CDOM absorption spectra were featureless in the UV and only those sampled in autumn showed the absorption bump around 310–320 nm. This suggests that the absorption bump around 310–320 nm could be a consequence of MAAs release into seawater by picophytoplankton after the bloom, plausibly as an effect of cell lysis (Whitehead and Vernet, 2000) or through exudates in response to environmental stress factors (Oren, 1997; Whitehead and Vernet, 2000).

3.7. Bio-optical relationships

No relationship was observed between S_{cdom} and [Tchl a+pheo a] over the BOUSSOLE time-series when all samples from the 0–400 m water column were considered (Fig. 10a). This is consistent with previous observations in the Mediterranean Sea (Bracchini et al., 2010) and the Southeast Pacific Ocean (Bricaud et al., 2010). When analyzing surface samples only, S_{cdom} values varied as a function of [Tchl a+pheo a] concentrations but with very high scatter (r^2=0.28, $p<0.01$, n=34; Fig. 10b).

The a_{cdom}(440) values were loosely related to [Tchl a+pheo a] in the 0–400 m depth layer (r^2=0.289, $p<0.001$, n=210; Fig. 10c). The low correlation and the large scatter in this relationship can be partly attributed to the time shift between CDOM and chlorophyll maxima (discussed in Section 3.5), which leads for instance to a number of situations with simultaneous high [Tchl a+pheo a] concentrations and low a_{cdom}(440) values (e.g., the period of the algal bloom).

Surface a_{cdom}(440) showed a trend to increase with [Tchl a+pheo a] concentrations, but the scatter was large (r^2=0.293, n=34, $p<0.001$; see Fig. 10d). Almost all points in Fig. 10d stood above the relationships proposed by Morel and Gentili (2009a) and Bricaud et al. (2010). The former was derived from a global bio-optical model, and the latter from in situ measurements collected in the Southeast Pacific Ocean. The main reason is the higher-than-average contribution of CDOM for a given chlorophyll content in the Mediterranean in contrast to other oceans (Morel and Gentili, 2009b). Note that the BOUSSOLE data set includes all seasons and encompasses situations with varying influences of photobleaching, which likely explains a large part of the data scatter in Fig. 10d.

3.8. Light absorption budget

The relative contributions of CDOM, phytoplankton and non-algal particles to the total non-water light absorption at 440 nm are shown for the BOUSSOLE time-series in Fig. 11. Over two years of measurements, and all along the water column, the CDOM contribution to the light absorption budget varied from 19 to 88% with an average value of 54 ± 15%. Similarly to other oceanic regions (Bricaud et al., 2002, 2010), CDOM was the only dominant light-absorbing substance in the layer below the DCM (Fig. 11a). From the surface to the DCM, CDOM contributed from a minimum of about 25% up to about 70% (Fig. 11a). The relative contribution of phytoplankton absorption was on average 33 ± 17%, with the lowest contributions (< 40%) below the DCM and values up to 70% above it (Fig. 11b). The non-algal particles were a minor

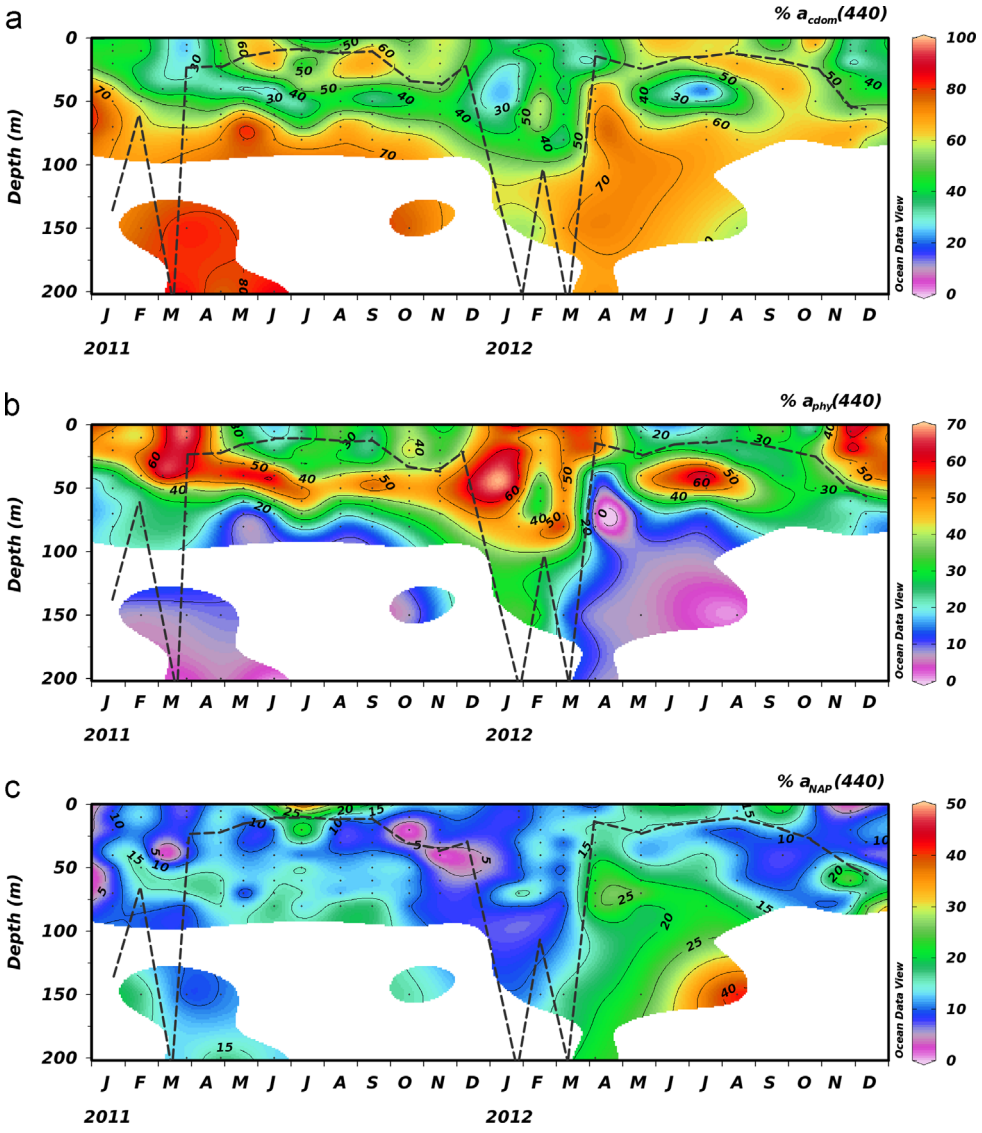

Fig. 11. Contour plots of relative contributions to total non-water light absorption at 440 nm of: (a) CDOM; (b) phytoplankton; (c) non-algal particles. Data are displayed within 0–200 m ($n=178$) for the period from January 2011 to December 2012. Small dots represent samples collected during each cruise and the dashed line indicates the Mixed Layer Depth (MLD).

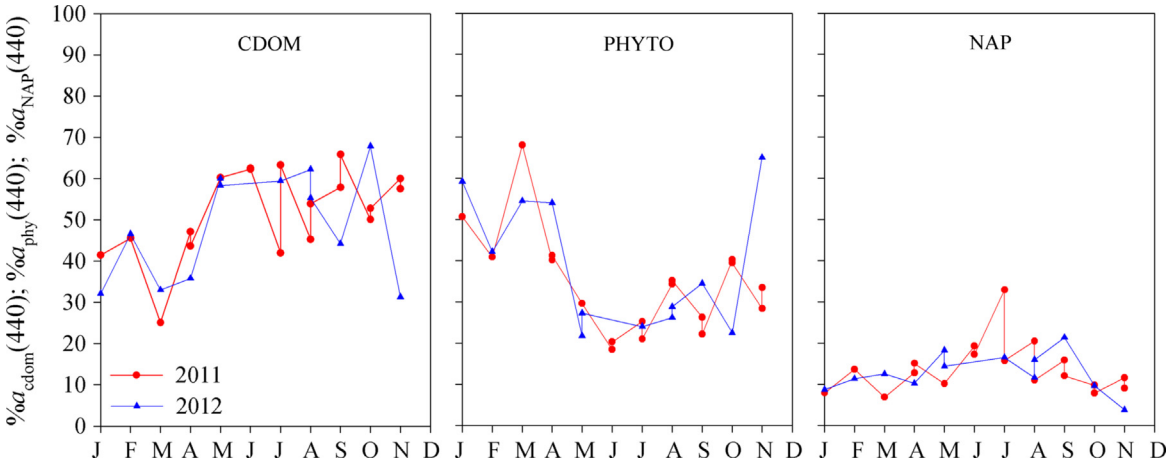

Fig. 12. Annual cycle of the relative contributions of CDOM, phytoplankton and non-algal particles to total non-water light absorption at 440 nm within the first optical depth at the BOUSSOLE site.

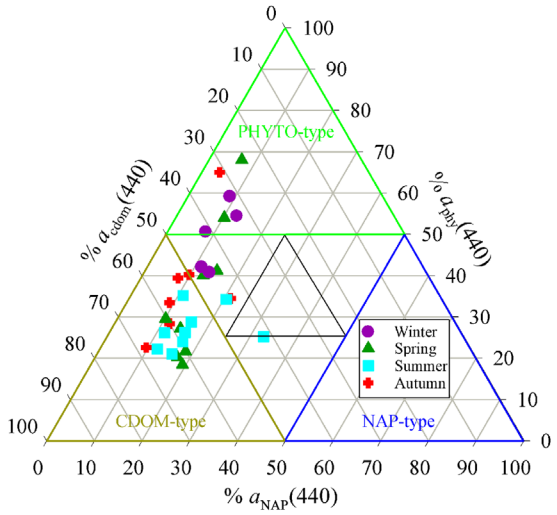

Fig. 13. Relative contributions of CDOM, phytoplankton and non-algal particles to total non-water light absorption at 440 nm within the first optical depth at the BOUSSOLE site in 2011 and 2012 ($n=30$). Boundaries of the optical classification for different types of water (Prieur and Sathyendranath, 1981) are displayed as coloured lines. (For interpretation of the references to color in this figure legend, the reader is referred to the web version of this article.)

component in the non-water light absorption budget (average value of $13 \pm 6\%$; Fig. 11c).

Temporal dynamics of CDOM, phytoplankton and non-algal particles relative contributions to total non-water light absorption within the first optical depth is displayed in Fig. 12. In this layer of importance for remote sensing applications, non-algal particles were the minor component of the absorption budget, with no specific seasonal dynamics. The contribution of non-algal particles to Colored Detrital Matter (CDM) was also generally weak (11 to 44%, with an average value of $21 \pm 7\%$; $n=30$). Phytoplankton was the major absorbing substance only during the bloom in March and April, whereas CDOM absorption dominated the rest of the year. This dominance even held in summer when the CDOM absorption was minimal as a consequence of photobleaching. Hence, during most of the year with the exception of the algal bloom in March and April, surface waters at BOUSSOLE can be classified as "CDOM-type" waters (Fig. 13) according to the optical classification proposed by Prieur and Sathyendranath (1981). Although such a classification could suggest that surface waters at the BOUSSOLE site are Case-2 waters, it is important to keep in mind that CDOM at the BOUSSOLE site has a local and biologically-driven origin, and its concentration varies, although with high scatter, with algal biomass (Fig. 10d). This means that surface waters at the BOUSSOLE site must be considered as Case-1 waters according to the definition of Morel and Prieur (1977), as already stated by Antoine et al. (2008).

4. Summary and conclusions

The analysis of a two-year time-series in the NW Mediterranean Sea revealed clear seasonal dynamics of CDOM light absorption coefficients and exponential slope values. The seasonal patterns observed in the 0–400 m layer at the BOUSSOLE site were consistent with those described for other oceanic regions, for example in the Sargasso Sea at the BATS site (Nelson and Siegel, 2013).

As discussed above, heterotrophic bacteria were likely the main source of CDOM in spring and summer. We found simultaneous maxima of CDOM and bacteria concentrations that lagged the algal bloom at the surface and DCM by about 1 month. CDOM destruction was, instead, driven by photochemical reactions. The CDOM photobleaching clearly appeared in the surface layer, especially in summer and autumn, when the lowest CDOM absorption coefficients and highest spectral slopes were observed. In particular, maximal spectral slope values lagged the maximal PAR values in June by about 3 months and this suggested that CDOM photoreactivity was more likely dependent on the time of exposure to light than on solar radiation rates.

Comparison of the relationship between CDOM absorption coefficients and chlorophyll concentrations with those found for other oceanic waters (Morel and Gentili, 2009a, Bricaud et al., 2010) revealed that the CDOM content at the BOUSSOLE site was above that expected for generally oligotrophic waters. This finding was consistent with the satellite study by Morel and Gentili (2009b) carried out over the entire Mediterranean basin where they supposed this notably high CDOM content to be essentially the effect of the strong vertical convective mixing characterizing this semi-enclosed sea. This high CDOM content strongly affected, as a consequence, the total non-water light absorption budget at the BOUSSOLE site.

It is intuitive that this largely dominant contribution of CDOM to light absorption in the blue might spectrally affect irradiance reflectance and remote sensing reflectance in the surface layer. This might cause the failure of globally-validated bio-optical models used for the retrieval of biogeochemical parameters (e.g., chlorophyll *a*) when applied to waters such as those characterizing the BOUSSOLE site or the Mediterranean Sea in general. In order to provide the ocean colour community with appropriate tools for working on these optical conditions, efforts are underway for testing the applicability and performances of current bio-optical models in retrieving CDOM, chlorophyll and other variables over the BOUSSOLE time-series and for working to their refinement. Thanks to the buoy permanently deployed at this site (Antoine et al., 2006), a consistent time-series of radiometric measurements recorded every 15 min night and day is actually available. This ongoing exercise will hopefully represent an important step for improving the prediction of CDOM and other biological quantities at the BOUSSOLE site and over the Mediterranean basin, so that the knowledge of the biogeochemical state and fluxes of organic matter in this semi-enclosed sea might be improved.

Acknowledgments

We thank Emilie Diamond, Melek Golbol and the captains and crews of the research vessels (*Téthys-II*, *Antea, Europe*) operating for monthly cruises. Joséphine Ras and Mustapha Ouhssain performed HPLC and particulate absorption measurements, Vincenzo Vellucci and Bernard Gentili helped in processing the PAR data. David Pecqueur and Christophe Salmeron (Observatoire Océanologique de Banyuls sur Mer, France) performed bacterial counts as part of the French national service of flow cytometry analyses. We also thank Xiaogang Xing and Hervé Claustre for sharing CDOM absorption data retrieved from the Bio-Argo float "MED_NW_B02" measurements. This study is a contribution to the BIOCAREX project, which was funded by the Agence Nationale de la Recherche (ANR), and to the BOUSSOLE project. We thank the multiple organizations that support BOUSSOLE and provide technical and logistic support: European Space Agency (ESA; Grant No: 4000102992/11/I-NB), Centre National d'Etudes Spatiales (CNES), Centre National de la Recherche Scientifique (CNRS), National Aeronautics and Space Administration (NASA), Institut National des Sciences de l'Univers (INSU), Université Pierre et Marie Curie (UPMC), Observatoire Océanologique de Villefranche sur Mer (OOV).

References

Andrew, A.A., Del Vecchio, R., Subramaniam, A., Blough, N.V., 2013. Chromophoric dissolved organic matter (CDOM) in the Equatorial Atlantic Ocean: optical properties and their relation to CDOM structure and source. Mar. Chem. 148, 33–43.

Antoine, D., Chami, M., Claustre, H., D'Ortenzio, F., Morel, A., Bécu, G., Gentili, B., Louis, F., Ras, J., Roussier, E., Scott, A.J., Tailliez, D., Hooker, S.B., Guevel, P., Desté, J.F., Dempsey, C., Adams, D., 2006. BOUSSOLE: A Joint CNRS-INSU, ESA, CNES and NASA Ocean Color Calibration and Validation Activity. NASA Technical Memorandum N° 2006-214147.

Antoine, D., D'Ortenzio, F., Hooker, S.B., Bécu, G., Gentili, B., Tailliez, D., Scott, A.J., 2008. Assessment of uncertainty in the ocean reflectance determined by three satellite ocean color sensors (MERIS, SeaWiFS and MODIS-A) at an offshore site in the Mediterranean Sea (BOUSSOLE project). J. Geophys. Res. 113, C07013, http://dx.doi.org/10.1029/2007JC004472.

Babin, M., Stramski, D., Ferrari, G.M., Claustre, H., Bricaud, A., Obolensky, G., Hoepffner, N., 2003. Variations in the light absorption coefficients of phytoplankton, nonalgal particles, and dissolved organic matter in coastal waters around Europe. J. Geophys. Res. 108 (C7), 3211, http://dx.doi.org/10.1029/2001JC000882.

Bracchini, L., Tognazzi, A., Dattilo, A.M., Decembrini, F., Rossi, C., Loiselle, S.A., 2010. Sensitivity analysis of CDOM spectral slope in artificial and natural samples: an application in the central eastern Mediterranean Basin. Aquat. Sci. 72, 485–498.

Bricaud, A., Babin, M., Claustre, H., Ras, J., Tieche, F., 2010. Light absorption properties and absorption budget of Southeast Pacific waters. J. Geophys. Res. 115, C08009, http://dx.doi.org/10.1029/2009JC005517.

Bricaud, A., Ciotti, A.M., Gentili, B., 2012. Spatial-temporal variations in phytoplankton size and colored detrital matter absorption at global and regional scales, as derived from twelve years of SeaWIFS data (1998-2009). Global Biogeochem. Cycles 26, GB1010, http://dx.doi.org/10.1029/2010GB003952.

Bricaud, A., Morel, A., Prieur, L., 1981. Absorption by dissolved organic matter of the sea (yellow substance) in the UV and visible domains. Limnol. Oceanogr. 26 (1), 43–53.

Bricaud, A., Roesler, C.S., Parslow, J.S., Ishizaka, J., 2002. Bio-optical studies during the JGOFS-equatorial Pacific program: a contribution to the knowledge of the equatorial system. Deep Sea Res. Part II 49, 2583–2599.

Bricaud, A., Stramski, D., 1990. Spectral absorption coefficients of living phytoplankton and nonalgal biogenous matter: a comparison between Peru upwelling area and Sargasso Sea. Limnol. Oceanogr. 35, 562–582.

Carder, K.L., Steward, R.G., Harvey, G.R., Ortner, P.B., 1989. Marine humic and fulvic acids: their effects on remote sensing of ocean chlorophyll. Limnol. Oceanogr. 34, 68–81.

Carreto, J.I., Carignan, M.O., 2011. Mycosporine-like amino acids: relevant secondary metabolites. Chemical and ecological aspects. Mar. Drugs 9, 387–446.

Coble, P.G., 2007. Marine optical biogeochemistry: the chemistry of ocean color. Chem. Rev. 107, 402–418.

Del Vecchio, R., Blough, N.V., 2002. Photobleaching of chromophoric dissolved organic matter in natural waters: kinetics and modeling. Mar. Chem. 78, 231–253.

Del Vecchio, R., Blough, N.V., 2004. Spatial and seasonal distribution of chromophoric dissolved organic matter and dissolved organic carbon in the Middle Atlantic Bight. Mar. Chem. 89, 169–187.

D'Ortenzio, F., Iudicone, D., de Boyer Montegut, C., Testor, P., Antoine, D., Marullo, S., Santoleri, R., Madec, G., 2005. Seasonal variability of the mixed layer depth in the Mediterranean Sea as derived from in situ profiles. Geophys. Res. Lett. 32, L12605, http://dx.doi.org/10.1029/2005GL022463.

Gordon, H.R., McCluney, W.R., 1975. Estimation of the depth of sunlight penetration in the sea for remote sensing. Appl. Opt. 14, 413–416.

Green, S.A., Blough, N.V., 1994. Optical absorption and fluorescence properties of chromophoric dissolved organic matter in natural waters. Limnol. Oceanogr. 39 (8), 1903–1916.

Helms, J.R., Stubbins, A., Ritchie, J.D., Minor, E.C., Kieber, D.J., Mopper, K., 2008. Absorption spectral slopes and slope ratios as indicators of molecular weight, source, and photobleaching of chromophoric dissolved organic matter. Limnol. Oceanogr. 53 (3), 955–969.

Hu, C., Lee, Z., Muller-Karger, F.E., Carder, K.L., Walsh, J.J., 2006. Ocean color reveals phase shift between marine plants and yellow substance. IEEE Geosci. Remote Sens. Lett. 3 (2), 262–266.

Kitidis, V., Stubbins, A.P., Uher, G., Upstill-Goddard, R.C., Law, C.S., Malcom, E., Woodward, S., 2006a. Variability of chromophoric organic matter in surface waters of the Atlantic Ocean. Deep Sea Res. Part II 53, 1666–1684.

Kitidis, V., Uher, G., Upstill-Goddard, R.C., Mantoura, R.F.C., Spyres, G., Woodward, E. M.S., 2006b. Photochemical production of ammonium in the oligotrophic Cyprus Gyre (Eastern Mediterranean). Biogeosciences 3, 439–449.

Marty, J.C., 2002. Preface to volume 49 number 11: DYFAMED time-series program (France JGOFS). Deep Sea Res. Part II, 1963–1964.

Marty, J.C., Chiavérini, J., Pizay, M.D., Avril, B., 2002. Seasonal and interannual dynamics of nutrients and phytoplankton pigments in the western Mediterranean Sea at the DYFAMED time-series station (1991-1999). Deep Sea Res. Part II 49, 1965–1985.

Maselli, F., Massi, L., Pieri, M., Santini, C., 2009. Spectral angle minimization for the retrieval of optically active seawater constituents from MODIS data. Photogramm. Eng. Remote Sens. 75 (5), 595–605.

Matsuoka, A., Bricaud, A., Benner, R., Para, J., Sempéré, R., Prieur, L., Bélanger, S., Babin, M., 2012. Tracking the transport of colored dissolved organic matter in the Southern Beaufort Sea: relationship with hydrographic characteristics. Biogeosciences 9, 925–940, http://dx.doi.org/10.5194/bg-9-925-2012.

Matsuoka, A., Huot, Y., Shimida, K., Saitoh, S.-I., Babin, M., 2007. Bio-optical characteristics in the Western Arctic Ocean: implications for ocean color algorithms. Can. J. Remote Sens. 33, 503–518.

Mitchell B.G., 1990. Algorithms for determining the absorption coefficient of aquatic particulates using the quantitative filter technique (QFT). Ocean Optics X, 137–148.

Mitchell, B.G., Bricaud, A., Carder, K., Cleveland, J., Ferrari, G., Gould, R., Kahru, M., Kishino, M., Maske, H., Moisan, T., Moore, L., Nelson, N., Phinney, D., Reynolds, R., Sosik, H., Stramski, D., Tassan, S., Trees, C., Weidemann, A., Wieland, J., Vodacek, A., 2000. Determination of spectral absorption coefficients of particles, dissolved material and phytoplankton for discrete water samples. In: Fargion, G.S., Mueller, J.L. (Eds.), Ocean Optics Protocols for Satellite Ocean Color Sensor Validation, Revision 2. NASA Technical Memorandum N° 2000-209966.

Mitchell, B.G., Kahru, M., Wieland, J., Stramska, M., 2002. Determination of Spectral Absorption Coefficients of Particles, Dissolved Material and Phytoplankton for Discrete Water Samples. NASA/TM-2002-210004/Rev3-Vol2, 231-257.

Mopper, K., Kieber, D.J., 2002. Photochemistry and cycling of carbon, sulfur, nitrogen and phosphorus. In: Hansell, D.A., Carlson, C.A. (Eds.), Biogeochemistry of Marine Dissolved Organic Matter.. Academic, San Diego, Calif, pp. 455–507.

Moran, M.A., Sheldon, W.M., Zepp, R.G., 2000. Carbon loss and optical property changes during long-term photochemical and biological degradation of estuarine dissolved organic matter. Limnol. Oceanogr. 45 (6), 1254–1264.

Morel, A., 1988. Optical modeling of the upper ocean in relation to its biogenous matter content (case I waters). J. Geophys. Res. 93, 10749–10768.

Morel, A., Gentili, B., 2009a. A simple band ratio technique to quantify the colored dissolved and detrital organic material from ocean color remotely sensed data. Remote Sens. Environ. 113, 998–1011.

Morel, A., Gentili, B., 2009b. The dissolved yellow substance and the shades of blue in the Mediterranean Sea. Biogeosciences 6, 2625–2636.

Morel, A., Maritorena, S., 2001. Bio-optical properties of oceanic waters: a reappraisal. J. Geophys. Res. 106, 7163–7180.

Morel, A., Prieur, L., 1977. Analysis of variations in ocean color. Limnol. Oceanogr. 22, 709–722.

Nelson, N.B., Carlson, C.A., Steinberg, D.K., 2004. Production of chromophoric dissolved organic matter by Sargasso Sea microbes. Mar. Chem. 89, 273–287.

Nelson, N.B., Siegel, D.A., 2002. Chromophoric DOM in the open ocean. In: Hansell, D.A., Carlson, C.A. (Eds.), Biogeochemistry of Marine Dissolved Organic Matter.. Academic, San Diego, Calif, pp. 547–578.

Nelson, N.B., Siegel, D.A., 2013. The global distribution and dynamics of chromophoric dissolved organic matter. Annu. Rev. Mar. Sci. 5, 447–476.

Nelson, N.B., Siegel, D.A., Carlson, C.A., Swan, C.M., 2010. Tracing global biogeochemical cycles and meridional overturning circulation using chromophoric dissolved organic matter. Geophys. Res. Lett. 37, L03610, http://dx.doi.org/10.1029/2009GL042325.

Nelson, N.B., Siegel, D.A., Carlson, C.A., Swan, C., Smethie Jr, W.M., Khatiwala, S., 2007. Hydrography of chromophoric dissolved organic matter in the North Atlantic. Deep Sea Res. Part I 54, 710–731.

Nelson, N.B., Siegel, D.A., Michaels, A.F., 1998. Seasonal dynamics of colored dissolved material in the Sargasso Sea. Deep Sea Res. Part I 45, 931–957.

Norman, L., Thomas, D.N., Stedmon, C.A., Granskog, M.A., Papadimitriou, S., Krapp, R.H., Meiners, K.M., Lannuzel, D., van der Merwe, P., Dieckmann, G.S., 2011. The characteristics of dissolved organic matter (DOM) and chromophoric dissolved organic matter (CDOM) in Antarctic sea ice. Deep Sea Res. Part II 58, 1075–1091.

Oren, A., 1997. Mycosporine-like amino acids as osmotic solutes in a community of halophilic cyanobacteria. Geomicrobiol. J. 14 (3), 231–240.

Organelli, E., Bricaud, A., Antoine, D., Uitz, J., 2013. Multivariate approach for the retrieval of phytoplankton size structure from measured light absorption spectra in the Mediterranean Sea (BOUSSOLE site). Appl. Opt. 52 (11), 2257–2273.

Ortega-Retuerta, E., Frazer, T.K., Duarte, C.M., Ruiz-Halpern, S., Tovar-Sánchez, A., Arrieta, J.M., Reche, I., 2009. Biogeneration of chromophoric dissolved organic matter by bacteria and krill in the Southern Ocean. Limnol. Oceanogr. 54 (6), 1941–1950.

Para, J., Coble, P.G., Charrière, B., Tedetti, M., Fontana, C., Sempéré, R., 2010. Fluorescence and absorption properties of chromophoric dissolved organic matter (CDOM) in coastal surface waters of the northwestern Mediterranean Sea, influence of the Rhône River. Biogeosciences 7, 4083–4103, http://dx.doi.org/10.5194/bg-7-4083-2010.

Prieur, L., Sathyendranath, S., 1981. An optical classification of coastal and oceanic waters based on the specific spectral absorption curves of phytoplankton pigments, dissolved organic matter, and other particulate materials. Limnol. Oceanogr. 26 (4), 671–689.

Ras, J., Uitz, J., Claustre, H., 2008. Spatial variability of phytoplankton pigment distributions in the Subtropical South Pacific Ocean: comparison between in situ and modelled data. Biogeosciences 5, 353–369.

Rochelle-Newall, E.J., Fisher, T.R., 2002. Chromophoric dissolved organic matter and dissolved organic carbon in Chesapeake Bay. Mar. Chem. 77, 23–41.

Romera-Castillo, C., Sarmento, H., Álvarez-Salgado, X.A., Gasol, J.M., Marrasé, C., 2010. Production of chromophoric dissolved organic matter by marine phytoplankton. Limnol. Oceanogr. 55 (1), 446–454.

Röttgers, R., Koch, B.P., 2012. Spectroscopic detection of a ubiquitous dissolved pigment degradation product in subsurface waters of the global ocean. Biogeosciences 9, 2585–2596.
Seritti, A., Russo, D., Nannicini, L., Del Vecchio, R., 1998. DOC, absorption and fluorescence properties of estuarine and coastal waters of the Northern Tyrrhenian Sea. Chem. Speciation Bioavailability 10 (3), 95–106.
Siegel, D.A., Maritorena, S., Nelson, N.B., Behrenfeld, M.J., McClain, C.R., 2005. Colored dissolved organic matter and its influence on the satellite-based characterization of the ocean biosphere. Geophys. Res. Lett. 32, L20605, http://dx.doi.org/10.1029/2005GL024310.
Siegel, D.A., Maritorena, S., Nelson, N.B., Hansell, D.A., Lorenzi-Kayser, M., 2002. Global distribution and dynamics of colored dissolved and detrital organic materials. J. Geophys. Res. 107 (C12), 3228, http://dx.doi.org/10.1029/2011JC000965.
Steinberg, D.K., Nelson, N., Carlson, C.A., Prusak, A.C., 2004. Production of chromophoric dissolved organic matter (CDOM) in the open ocean by zooplankton and the colonial cyanobacterium *Trichodesmium* spp. Mar. Ecol. Prog. Ser. 267, 45–56.
Swan, C.M., Nelson, N.B., Siegel, D.A., Kostadinov, T.S., 2012. The effect of surface irradiance on the absorption spectrum of chromophoric dissolved organic matter in the global ocean. Deep Sea Res. Part I 63, 52–64.
Swan, C.M., Siegel, D.A., Nelson, N.B., Carlson, C.A., Nasir, E., 2009. Biogeochemical and hydrographic controls on chromophoric dissolved organic matter distribution in the Pacific Ocean. Deep Sea Res. Part I 56, 2172–2192.
Tilstone, G., Airs, R., Martinez-Vicente, V., Widdicombe, C., Llewellyn, C., 2010. High concentrations of Mycosporine-like amino acids and coloured dissolved organic material in the sea surface microlayer off the Iberian Peninsula. Limnol. Oceanogr. 55 (5), 1835–1850.
Twardowski, M.S., Boss, E., Sullivan, J.M., Donaghay, P.L., 2004. Modeling the spectral shape of absorption by chromophoric dissolved organic matter. Mar. Chem. 89, 69–88.
Vignudelli, S., Santinelli, C., Murru, E., Nannicini, L., Seritti, A., 2004. Distributions of dissolved organic carbon (DOC) and chromophoric dissolved organic matter (CDOM) in coastal waters of the northern Tyrrhenian Sea (Italy). Estuarine Coastal Shelf Sci. 60, 133–149.
Vodacek, A., Blough, N.V., DeGrandpre, M.D., Peltzer, E.T., Nelson, R.K., 1997. Seasonal variation of CDOM and DOC in the Middle Atlantic Bight: terrestrial inputs and photooxidation. Limnol. Oceanogr. 42 (4), 674–686.
Whitehead, K., Vernet, M., 2000. Influence of mycosporine-like amino acids (MAAs) on UV absorption by particulate and dissolved organic matter in La Jolla Bay. Limnol. Oceanogr. 45 (8), 1788–1796.
Xing, X., Claustre, H., Wang, H., Poteau, A., D'Ortenzio, F., 2014. Seasonal dynamics in colored dissolved organic matter in the Mediterranean Sea: patterns and drivers. Deep Sea Res. Part I 83, 93–101.
Xing, X., Morel, A., Claustre, H., D'Ortenzio, F., Poteau, A., 2012. Combined processing and mutual interpretation of radiometry and fluorometry from autonomous profiling Bio-Argo floats: 2. Colored Dissolved Organic Matter absorption retrieval. J. Geophys. Res. 117, C04022, http://dx.doi.org/10.1029/2011JC007632.
Yamashita, Y., Nosaka, Y., Suzuki, K., Ogawa, H., Takahashi, K., Saito, H., 2013. Photobleaching as a factor controlling spectral characteristics of chromophoric dissolved organic matter in open ocean. Biogeosciences 10, 7207–7217.
Yamashita, Y., Tanoue, E., 2009. Basin scale distribution of chromophoric dissolved organic matter in the Pacific Ocean. Limnol. Oceanogr. 54, 598–609.